

Optimization of Spray Quenching for Aluminum Extrusion, Forging, or Continuous Casting

T.A. Deiters and I. Mudawar

Abstract. A review of the current understanding of heat transfer from quenched alloy products to water sprays is presented. A numerical example is described to demonstrate how controlled spray cooling of products containing sections of differing thicknesses significantly reduces thermal gradients. A semi-expert computer-aided design (CAD) system is proposed for optimizing the process of spray quenching following extrusion, forging, or continuous casting. A systematic experimental approach to the problem of providing a universal heat transfer data base for the proposed CAD system is presented.

INTRODUCTION

Mechanical and metallurgical requirements impose limits on the rates at which aluminum alloys can be quenched by water sprays. The upper limit is set by the occurrence of plastic deformation which causes warping of the product and the lower limit is set by an inability to develop the required metallurgical properties in subsequent heat treatment operations. In addition, if a product contains sections of differing thicknesses, it is unlikely that the optimum properties can be obtained throughout the entire cross section using a single spray density. At present a method for determining the nozzle configuration and spray density required for the spray cooling of a given alloy of given geometry is not available and this causes much guesswork and trial and error in establishing an acceptable configuration for a production run.

The transformation of bulk liquid into sprays and other physical dispersions of small particles in a gaseous atmosphere has importance in several industrial processes such as the application of chemicals to agricultural crops, paint spraying, spray drying of wet solids, food processing, cooling of nuclear cores, and dispersions of liquid fuels for combustion [1]. Of specific interest in the present work is the application of water sprays to the quenching of aluminum alloys.

Accurate control of the cooling rates during quenching requires a careful characterization of the spray. One means of characterizing the effectiveness of sprays is the boiling curve shown in Figure 1 as a log-log plot of the variation of the heat flux from a hot surface, q , with the difference between the temperature of the hot surface and the saturation temperature of the cooling fluid, ΔT_s . If, in a spray quenching process, the initial value of ΔT_s is high enough, the liquid droplets in the spray do not make contact with the surface. The phenomenon occurs in the film boiling regime of the boiling curve, corresponding to the location of point 1 in Figure 1. In this regime heat transfer to the spray is relatively poor because of the insulating properties of the thin blanket of vapor which is produced on the hot surface. With continued cooling both the heat flux and the surface temperature decrease until a minimum in the former is reached at the Leidenfrost point, located at position 2 in Figure 1. At this point liquid droplets in the spray begin to penetrate to the metal surface and a transition to nucleate boiling within the drops commences. With further decrease in ΔT_s , the heat flux increases as the regime of nucleate boiling is entered, and at the onset of full nucleate boiling the heat flux from the surface reaches a maximum value, called the critical heat flux, at point 3 in Figure 1. With further cooling of the surface, nucleate boiling ceases and heat transfer occurs by single-phase convection to the cooling water flowing over the surface. Consequently, in this regime of forced convection, a decrease in ΔT_s causes a decrease in the heat flux, as shown at location 4 in Figure 1.

T.A. Deiters is Graduate Research Assistant and I. Mudawar is Assistant Professor and Director of the Boiling and Two-Phase Flow Laboratory, School of Mechanical Engineering, Purdue University, West Lafayette, IN 47907, USA.

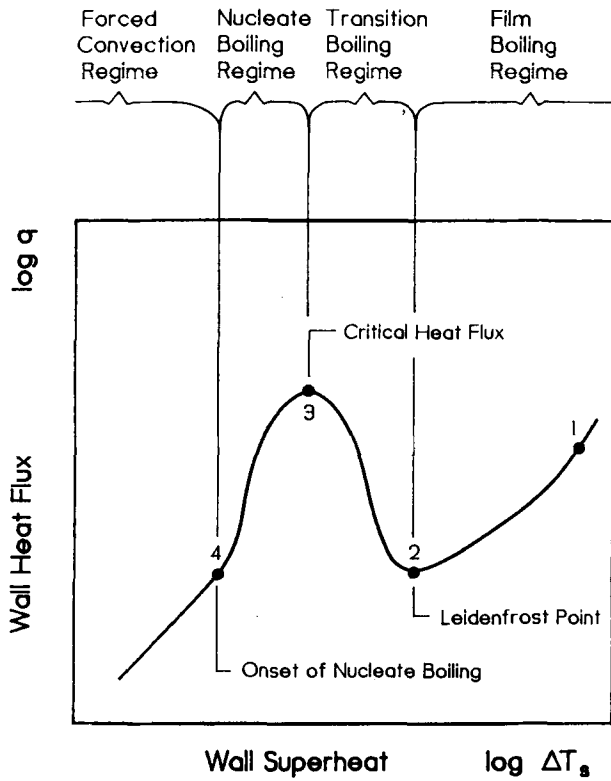


Fig. 1. Boiling curve.

Although the quench curve has been studied by many investigators, the criteria governing the positions of the critical heat flux and the Leidenfrost temperature are not well understood. Since, for any given cooling medium, the Leidenfrost temperature is that below which the quench rate of the surface begins to increase rapidly, knowledge of the Leidenfrost temperature is critical to accurate control of cooling rates during quenching.

An alternative approach to studying the quenching process is to determine the variation of the temperature at a specific location on the surface with time, and a typical variation is shown in Figure 2. The changes in the slope of the curve with time arise from the transition from one cooling regime to another. During initial film boiling, which occurs up to time t_2 , the rate of cooling is low because of the insulating properties of the vapor blanket formed on the surface. At T_2 , which is the Leidenfrost point, film boiling is interrupted by partial liquid–solid contact and the rate of cooling increases significantly until the critical heat flux condition is reached at T_3 after time t_3 . After t_4 , nucleate boiling is replaced by forced convection and the rate of cooling decreases accordingly.

Although Figures 1 and 2 clearly show the different regimes of heat transfer associated with spray cooling, the actual forms of the curves can be influ-

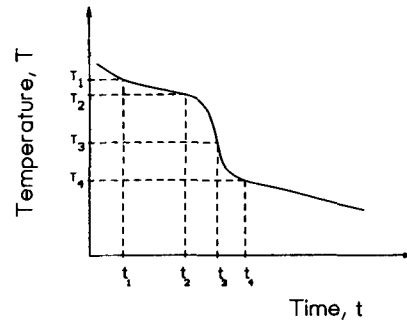


Fig. 2. Transient temperature variation of a quenched alloy product.

enced by external parameters such as surface roughness and spray hydrodynamics. For example, with a heavy enough spray density, it is possible that the regime of film boiling can be avoided during the quenching of aluminum. In addition, the curves in Figures 1 and 2 are for a single location on a surface. Thus, if a part being quenched has an irregular shape, or contains sections of differing thicknesses, an industrial quench can cause variations in the local quench rates. This can have a serious influence on the mechanical and metallurgical properties of quenched aluminum alloys.

The influence of quench rate on the metallurgical properties of age-hardening Al–Cu alloys can be explained by reference to the Al–Cu phase diagram shown in Figure 3. When an alloy of composition C_0 , which at 500° C is a solid solution of Cu in Al, is cooled to its solvus temperature, T_1 , the solid solution becomes saturated with Cu. Cooling below T_1 causes precipitation of the intermetallic θ phase, CuAl_2 , and the mechanical properties of the alloy are determined by the morphology of the precipitates in the primary solid solution. As precipitation is a rate process, a sufficiently fast quench of the alloy through the solvus

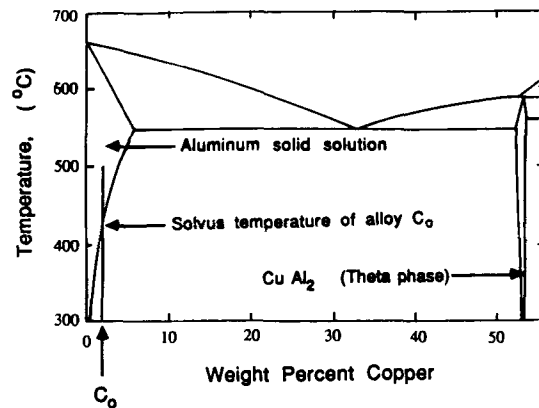


Fig. 3. The aluminum–copper phase diagram.

temperature to room temperature can suppress all precipitation and produce a homogeneous supersaturated solid solution. Subsequent age hardening of this alloy produces an even dispersion of very fine precipitates which imparts the desired maximum strength and hardness to the alloy. On the other hand, slow cooling from the solvus temperature causes massive precipitation at the grain boundaries during cooling and produces a structure which cannot be age hardened. This structure possesses minimum strength and minimum hardness. For any alloy there thus exists a minimum quench rate above which precipitation of the θ phase is suppressed. However, because the yield strengths of metals decrease with increasing temperature, a maximum quench rate occurs above which the temperature gradients developed are sufficient to produce plastic deformation of the metal. This causes warping. At the present time there is no systematic way of predicting the transient behavior of quenched metal objects and, consequently, a costly trial and error approach must be used to produce alloy products of acceptable quality.

The existence of upper and lower limits on quenching rates, which define an acceptable "hardenability window" has been considered by Chevier et al. [2]. Figure 4 shows, schematically, the variation of cooling rate, dT/dt , with temperature T during a quench. The broken line, a, shows the maximum quench rate above which plastic deformation of the metal will occur and the horizontal broken line, b, shows the minimum quench rate below which precipitation of the θ phase will begin at the solvus temperature T_2 and continue until the temperature T_1 (the temperature at which the kinetics of precipitation become vanishingly small) is reached. Lines a and b define the acceptable "hardenability window." The full line 1 is drawn for a cold water quench and, as this curve lies above curve a, the quench will cause plastic deformation and mechanical distortion. The full line 2 is drawn for a quench

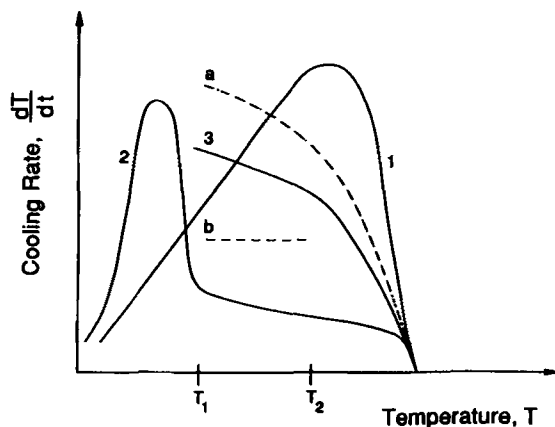


Fig. 4. Window of acceptable cooling rates [2].

in boiling water and, as this lies below line b, age hardening will not develop the desired mechanical properties. An ideal quench, which passes through the hardenability window, is shown by line 3.

Achievement of a quench rate, such as given by line 3, using water sprays requires a fundamental understanding of the parameters governing heat transfer. Brimacombe et al. [3] have reviewed the literature on spray cooling and have attempted to develop a general design method for the spray cooling of continuously cast steel. All of the studies reviewed concluded that the volumetric spray flux, \dot{Q} , has the largest effect on the heat transfer coefficient, but contradiction occurs when knowledge of the critical secondary parameters is required. Bolle and Moreau [4, 5] have suggested that, in the film boiling regime, the effect of surface temperature can be neglected without sacrificing acceptable accuracy. This is in contrast with Sasaki et al. [6] who concluded that the dependence on temperature in the film boiling regime is significant, and they included it in their correlation of the spray heat transfer coefficient. Muller and Jeschar [7] are the only investigators to have included the velocity of the water at the orifice of the nozzle in the correlation. Some of the controversy can be resolved by an examination of the ranges over which the parameters were allowed to vary. In pressure sprays used in the materials processing industry, drop velocities can range from 0.4 to 30 m/s. Muller and Jeschar, whose study included velocities in the range 10–30 m/s, included velocity in their correlation. It is possible that the other studies did not find velocity to be important because of the low range of values over which they were studied. Urbanovich et al. [8] found that, although the heat transfer coefficient was increased by moving the nozzle closer to the surface, this also increased the nonuniformity of the heat transfer across the surface. Nonuniformity has been supported by Reiners et al. [9] who observed a change of 2000 W/m²K in the heat transfer coefficient over a distance of 100 mm.

Most of the studies of spray quenching have been concerned with the cooling of steel from very high temperatures and, consequently, most of the conclusions drawn pertain to the film boiling regime, which, as shown in Figures 1 and 2, is a slow cooling process. In the spray cooling of aluminum alloys the surface temperatures may be only slightly higher than the Leidenfrost point, and, with some powerful sprays, even lower than this point. It is thus necessary that the entire boiling curve for aluminum be determined.

NOMENCLATURE

The following nomenclature is used throughout this paper.

- c_p = specific heat of alloy at constant pressure (J/kg K)
- d = drop diameter (mm)
- h = convection coefficient (W/m²K)
- k = thermal conductivity of alloy (W/m K)
- P = pressure (kPa)
- q = local heat flux (W/m²)
- \dot{Q} = local volumetric spray flux (m³s⁻¹/m²)
- t = time (s)
- T = temperature (°C)
- $\Delta T_s = T_s - T_{sat}$ (°C)
- u = drop velocity at impingement (m/s)
- ρ = density of alloy (kg/m³)

Subscripts

- f = inlet water conditions
- i = initial
- s = metal surface
- sat = saturation

CONTROLLED SPRAY COOLING CONCEPT

Using the limited results of previous studies, numerical simulation of the spray quenching of an aluminum product can clearly illustrate the feasibility of improving product quality by controlling the quench boundary between the product and the spray. A simple, yet inclusive, geometry was selected to simulate an aluminum extrusion during the quenching process. A schematic of the shape, and all relevant information, are shown in Figure 5. This specific profile was chosen because its thick thin ratio makes it an excellent candidate for deformation if it is quenched with a uniform bank of sprays.

It was assumed that the work piece was homogeneous and that the material properties remain constant

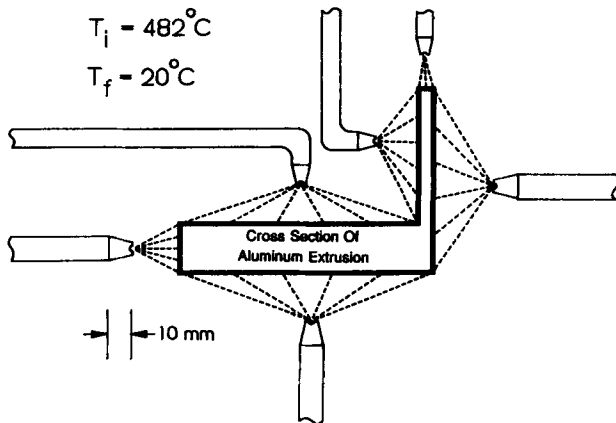


Fig. 5. Aluminum extrusion geometry utilized in the numerical verification of the controlled quenching system.

over the temperature range considered (482° C–50° C). The water spray was specified to be at a constant temperature of 20° C and the aluminum cross section was initially at a uniform temperature of 482° C. Heat loss due to radiation and axial conduction were neglected in this simplified two-dimensional analysis. The governing equation for this problem is:

$$\frac{\partial}{\partial t} (\rho c_p T) = \frac{\partial}{\partial x} \left(k \frac{\partial T}{\partial x} \right) + \frac{\partial}{\partial y} \left(k \frac{\partial T}{\partial y} \right) \quad (1)$$

and the boundary conditions are:

$$k \frac{\partial T}{\partial x} = q = h(T_s - T_f) \quad (2)$$

$$k \frac{\partial T}{\partial y} = q = h(T_s - T_f) \quad (3)$$

The heat flux results obtained by Bratuta and Kravtsov [10] and shown in Figure 6 were used to provide an estimate of the boundary conditions to be encountered with water sprays. The surface heat flux was measured as a function of surface temperature for three different spray fluxes (heavy, medium, and light). The figure shows that the heat flux (and thus the heat transfer coefficient) increases with an increase in volumetric spray flux. The heat flux values were converted to convection coefficient data by the definition:

$$q = h(T_s - T_f) \quad (4)$$

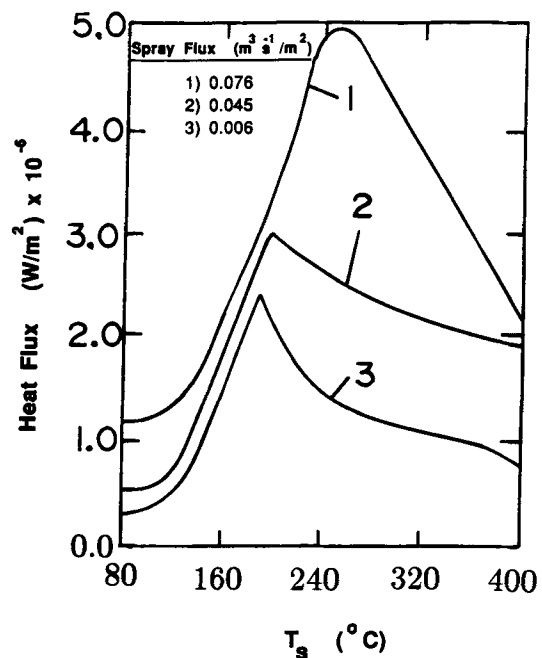


Fig. 6. Dependence of heat flux on spray density [10].

A finite difference program was used to calculate the transient temperature distribution in the cross section. A nonuniform grid, consisting of 200 nodes, was designed to give a high resolution of the temperature field in the area where the two legs joined as it was anticipated that the most severe thermal gradients would exist at this location.

The first numerical example shows the effects of a fast quench in which the highest spray density was used at each of the six surfaces, and Figure 7(a) shows a plot of the transient temperature at various locations in the cross section. The curves labeled C_1 , C_2 , and C_3 show the temperatures along the thin leg and the other curves are for the thick leg. Using this uniform spray boundary, the cooling envelope encompasses a 325°C temperature variation at one particular instant in time.

The large gap exhibited by the cooling envelope in Figure 7(a) indicates the temperature gradients which are developed in the part during the fast quench. The extruded angle has the dimension 10 cm by 7.5 cm and thus the predicted 325°C temperature gradient across this small part is destructive because it can cause residual stresses which, in turn, can cause warpage or

surface cracks. It is also important to note that the thin leg cools faster than the thick leg. To improve cooling uniformity, it is necessary to either increase the cooling rate of the thick leg to match that of the thin one or decrease the quench of the thin leg to that of the thick one. In practice this decision would be made using the window of acceptable cooling rates (Fig. 4) as a guideline. In the simulation, the quench rate of the thin leg was decreased because the boundary data from Bratuta and Kravtsov [10] were only available for lower spray fluxes.

A comparative simulation was run representing the "optimum" quench rate. The lowest spray flux density was used along the sides of the thin leg and on the end of the thick leg and the highest spray flux density was used along the top and bottom surfaces of the thicker one. The result of these boundary conditions, shown in Figure 7(b), was to shrink the cooling envelope from 325°C to 75°C . If the available data base had included higher density sprays the simulation could have included the case in which both legs were cooled at the same rate. A faster quench (provided it did not exceed the upper limit) would ensure the required hardness and the controlled cooling

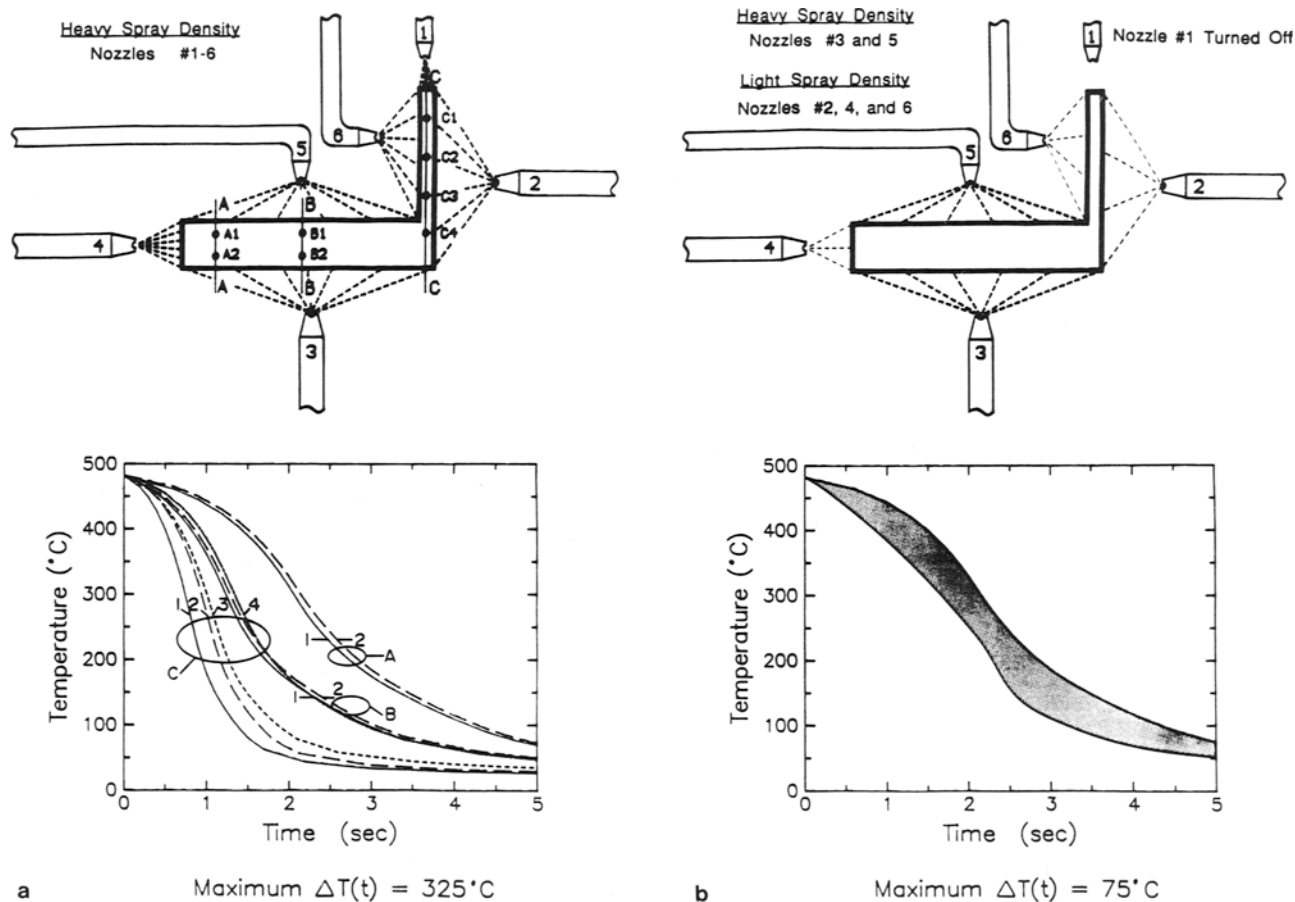


Fig. 7. Cooling history for an extrusion quenched with (a) uniform spray and (b) controlled spray.

would still protect the product from any surface cracks or deformation.

The results of the numerical simulation might be made even more accurate by including axial conduction effects. In addition, it is known that the heat transfer coefficient associated with sprays is a function of such independent parameters as spray flux, drop diameter, drop velocity, surface temperature, and liquid temperature and it is also known that these parameters may exhibit significant spatial variation within the spray field. Therefore it must be concluded that the heat transfer coefficient will vary spatially within the spray field. An accurate simulation should take into account this variation and not assume that the convection coefficient has the same relationship with temperature everywhere in the spray field. Although numerical simulation has shown that it is possible to adequately (and accurately) control the quenching process, insufficient heat transfer data for water sprays is a major obstacle to realizing this objective.

PROPOSED CONTROLLED QUENCH TECHNOLOGY

To improve quality and consistency between production runs and reduce costs, a method for optimizing the cooling rate for a particular shape and material is needed. The proposed approach involves the synthesis via CAD/CAM of heat transfer and materials engineering. As shown in Figure 8, an operator would input to a CAD system the geometry and desired properties of the part. The intelligent system would consult its materials data base to determine the cooling rate needed to produce parts with the desired metallurgical properties. It would then numerically solve for the transient temperature distribution in the metal piece using the heat transfer data base to provide the boundary conditions. The CAD system would iterate here several times until a set of boundary conditions

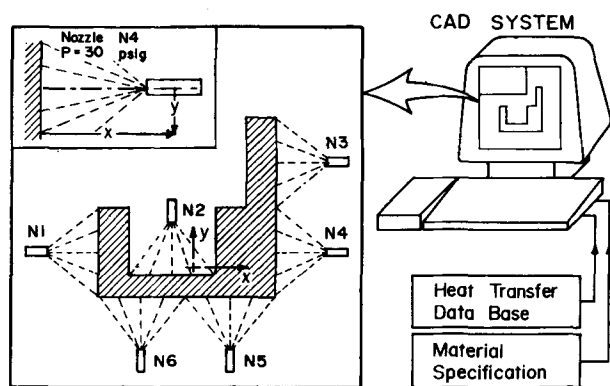


Fig. 8. Schematic of the proposed intelligent spray quenching system.

were found that provide a uniformly quenched product. These boundary conditions would be related to specific nozzle locations and pressures. The CAD system would then output these results to the operator who would prepare the quench chamber in accordance with the optimized recommendation. Possibly a microprocessor could robotically control the spray nozzle position and flow rate to further enhance the heat treatment process.

Even without the robot control this process is ideal for economizing the metal quenching industry. Initially, it will significantly decrease the costly set-up time and reduce the scrap material involved with the trial and error method of finding the correct quench rate. During production it provides consistent material properties by inhibiting the variability of product properties associated with day-to-day human decisions. Finally the post-treatment of the part to correct any distortions that may have occurred during the quench has virtually been eliminated. Additionally this process method is particularly well suited for small batch operations where pre- and post-production costs are not as easily recovered in the volume of parts produced.

The proposed controlled spray cooling system described in Figure 8 lacks a universal heat transfer data base that is needed to provide accurate boundary conditions for the numerical model utilized in the CAD software. It is known that the heat transfer coefficient can vary significantly within a spray field. The approach currently employed at Purdue's Boiling and Two-Phase Flow Laboratory is to investigate the local spray parameters such as volumetric spray flux, \dot{Q} , the drop velocity, u , and drop diameter, d , to determine what effects these parameters have on h , the local heat transfer coefficient. The next step will be to mathematically model the two-dimensional spatial variation of \dot{Q} , u , d , and h . As shown in schematic form in Figure 9, it is anticipated that the highest values of these parameters will be directly below the nozzle and then possibly follow a Gaussian distribution out to the spray boundaries. This formulation in addition to being a function of the X and Y coordinates is also dependent on the surface-to-nozzle distance and nozzle pressure. The advantage of having a mathematical model is that it greatly reduces the discrete data points that need to be taken in order to characterize the spray field. The nozzle manufacturer could make discrete measurements of \dot{Q} , u , and d at the locations shown in Figure 9 for specified nozzle pressures and heights above the sprayed surface. Using the mathematical model these measurements could be extrapolated to define the entire spray field in terms of \dot{Q} , u , and d . Then using the universal correlation of h with \dot{Q} , u , and d , the full spray field can

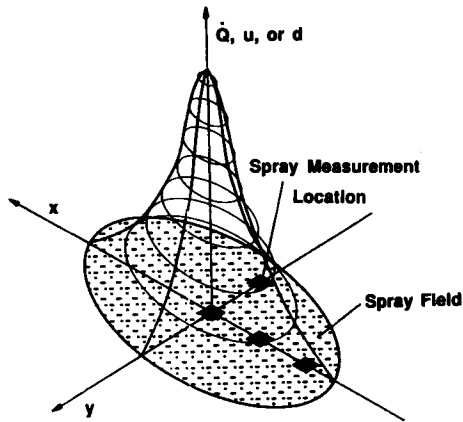


Fig. 9. Spatial variation of hydrodynamic spray parameters.

be characterized in terms of h , which defines the boundary condition for the numerical conduction problem.

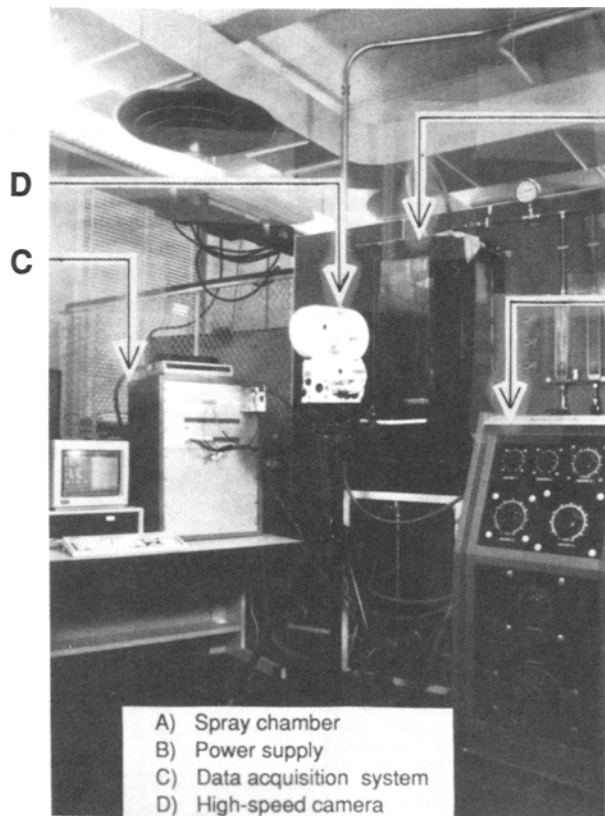
EXPERIMENTAL APPROACH

A research facility has been designed and installed in the Boiling and Two-Phase Flow Laboratory. The facility consists of a unique and effective system for

testing the heat transfer characteristics of sprays. The three primary components of the facility are the flow loop, the heated surface that simulates the quenched product, and the instrumentation.

Except for the test chamber, which is made of inert plastics, the fluid in the flow loop is circulated through stainless steel plumbing components. As shown in Figure 10 the loop starts with a 30 gal reservoir at the lower section of the test chamber. In order to achieve a broad data base, fluid temperatures up to saturation must be studied. The fluid drains from the reservoir to the pump which can deliver 4.45 gpm at 100 psi and can handle temperatures up to 100° C. The heat exchanger is used to cool and maintain the fluid at the desired test temperature. A filter is added to insure fluid purity. The flow rate is adjusted by the primary control valve which controls the flow rate to the nozzle, and a bypass valve which routes liquid back to the reservoir. The two rotameters cover overlapping flow rate ranges of 0.145–1.45 gpm and 0.628–6.28 gpm for accurate measurement at both low and high flow rates. The nozzle back pressure is determined by a dial pressure gauge as the fluid enters the test chamber, passes through the spray nozzle, and impinges on the heated surface.

The quench chamber is designed to maximize vi-



A

B

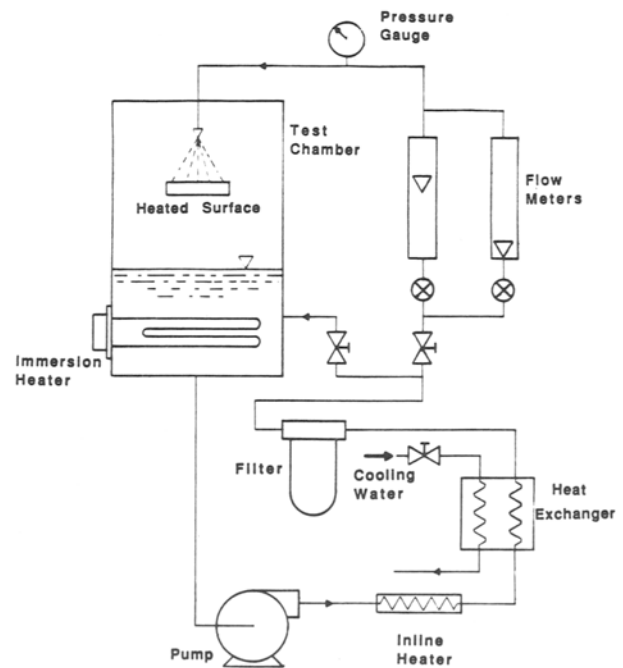


Fig. 10. Overall view of the spray cooling facility and a schematic of the flow loop.

sual access to the spray via three polycarbonate windows. Two photographic systems are used to aid in the understanding of spray interaction with the hot surface. The first is a low speed video system used for monitoring global spray characteristics. The second is an (NAC) high speed film based camera capable of exposure speeds of 40,000 partial frames per second. The NAC system is equipped with a long range Questar microscopic lens for close-up viewing of the deformation of single droplets as small as 2 μm in diameter upon impingement onto the surface.

A local, steady-state heat flux measurement technique was adopted in the present study. This allows for a detailed mapping of the heat flux distribution within the spray field. This technique was preferred to quenching a large preheated sample of alloy and obtaining an average heat transfer coefficient for the spray since the transient technique compromises accuracy in measuring the instantaneous surface heat flux during the transient and in detecting spatial variation in heat flux. As shown in Figure 11, the simulated test sample is machined into a circular calorimeter bar with one surface exposed to the spray while the back section is heated by three cartridge heaters. Four equally spaced chromel–alumel thermocouples made from 0.075 mm wire are embedded along the axis of the calorimeter bar. The design of the test sample was numerically optimized to ensure one-dimensional heat flow to the 50 mm² quenched surface area. Heat flux is determined from the linear temperature gradient between the four thermocouples, while the surface temperature is determined by extrapolating the temperature distribution along the axis. The test sample is mounted in a large insulating module designed to reduce heat loss from the heated sample.

A Compaq Deskpro 386 microcomputer is used in conjunction with a Keithley 500 data acquisition system to monitor temperatures in the heater and flow

loop. The data acquisition system also keeps track of the voltage and current input to the heater core.

As shown in Figure 12, the quench chamber is fitted with a three degree of freedom translation stage on which the spray nozzle is mounted. The simulated heater is placed at the geometric center of the spray chamber while the nozzle is positioned at any desired point relative to the heater in the X–Y–Z coordinate system to facilitate local measurements of the heat transfer coefficient throughout the spray field.

Figure 13 shows a three-dimensional plot of the

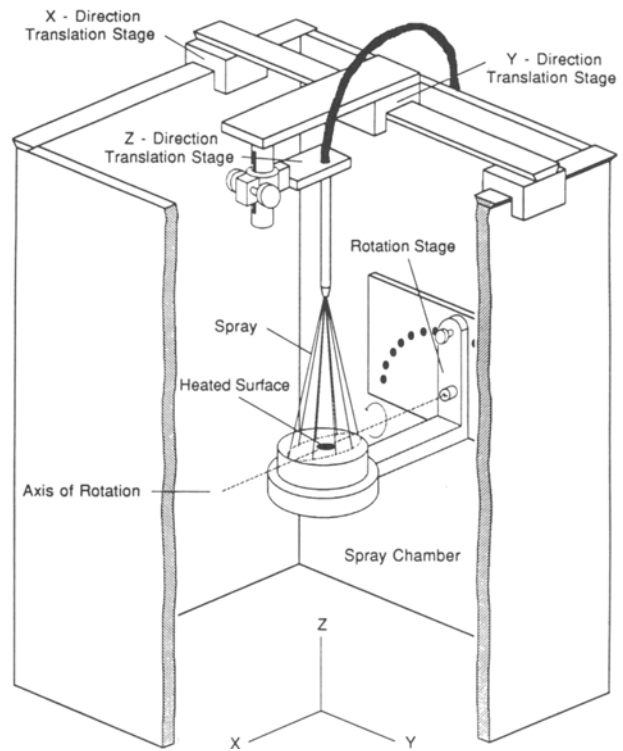


Fig. 12. Schematic of the quench chamber.

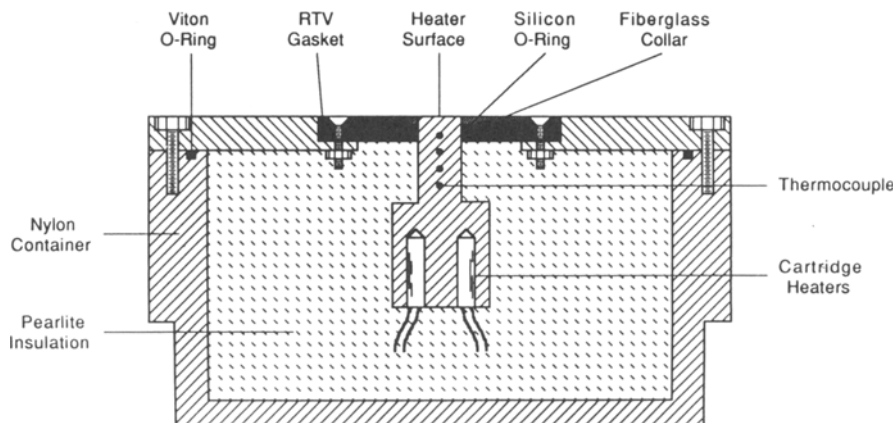


Fig. 11. Heater construction.

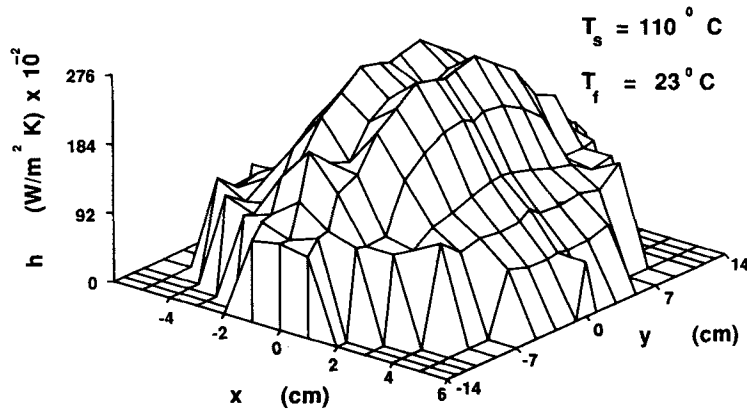


Fig. 13. Measured heat transfer coefficient as a function of position on the hot surface.

spatial variation of the measured heat transfer coefficient, h , with the spray field for fixed values of \dot{Q} , u , d , T_s , and T_f . These measurements confirm earlier findings by Urbanovich et al. [8] and Reiners et al. [9] concerning the nonuniformity of the heat transfer coefficient across the surface and the need for careful mapping of this behavior in predicting transient temperature variations in alloys during quenching, forging, or continuous casting.

Figure 14 shows a sample of the heat transfer data required for the CAD software. By selecting different spray nozzles, nozzle pressures, or nozzle-to-surface distances, it is possible to correlate the variation of surface heat flux (from which the convection heat transfer coefficient can be deduced) with respect to each of the primary parameters associated with the quenching process. A universal data base is then generated by combining all these parametric correlations. Since these correlations are based on local measure-

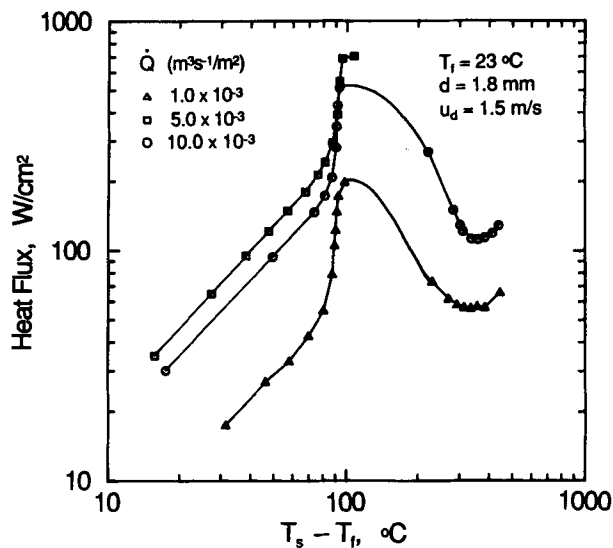


Fig. 14. Measured heat flux versus surface superheat for three spray fluxes.

ments, they could then be applied to any type of spray for which the variations of \dot{Q} , u , and d have been established.

ACKNOWLEDGMENT

Financial support of this work by a grant from the Computer Integrated Design, Manufacturing and Automation Center (CIDMAC) of Purdue University is gratefully acknowledged. The authors also thank Messrs. Gerry Dail and William Arthur of ALCOA and Mr. Jerry Hagers of Spraying Systems Co. for their technical assistance.

REFERENCES

1. A.L. Lefebvre, 1988, *Atomization and Sprays*, Hemisphere Pub. Corp., New York.
2. J. Chevier, A. Simon, and G. Beck, 1981, "Optimal Cooling Rate and Process Control in Metallic Parts Heat Treatment," In *Heat and Mass Transfer in Metallurgical Systems*, B. Spalding, ed., Hemisphere Pub. Corp., New York.
3. J.K. Brimacombe, P.K. Agarawal, L.A. Baptista, S. Hibbins, and B. Prabhakar, 1980, "Spray Cooling in the Continuous Casting of Steel," *63rd National Open Hearth and Basic Oxygen Steel Conf. Proc.*, Vol. 63, Washington, DC, pp. 235-252.
4. L. Bolle, and J.C. Moureau, 1976, "Spray Cooling of Hot Surfaces: A Description of the Dispersed Phase and a Parametric Study of Heat Transfer Results," *Proc. of Two Phase Flows and Heat Transfer*, Vol. III, NATO Advanced Study Institute, pp. 1327-1346.
5. L. Bolle and J.C. Moureau, 1979, "Experimental Study of Heat Transfer by Spray Cooling," *Proc. of Int. Conf. on Heat and Mass Transfer Metallurgical Processes*, Dubrovnik, Yugoslavia, pp. 527-534.
6. K. Sasaki, Y. Sugitani, and M. Kawasaki, 1979, "Heat Transfer in Spray Cooling on Hot Surface," *Testu-To-Hagane*, Vol. 65, pp. 90-96.
7. H. Muller and R. Jeschar, 1973, "Untersuchung des Wärmeübergangs an einer simulierten Sekundärkühl-

- zone beim Stronggiessverfahren," *Arch. Eisenhüttenwes*, Vol. 44, pp. 589–594.
8. L.I. Urbanovich, V. Goryainov, V. Sevost'ynov, Y. Boev, V. Niskovskikh, A. Grachev, A. Sevost'yanov, and V. Gur'ev, 1981, "Spray Cooling of High-Temperature Metal Surfaces with High Water Pressures," *Steel in the USSR*, Vol. 11, pp. 184–186.
 9. U. Reiners, R. Jeschar, R. Scholz, D. Zebrowski, and W. Reichelt, 1985, "A Measuring Method for Quick Determination of Local Heat Transfer Coefficients in Spray Cooling Within the Range of Stable Film Boiling," *Steel Research*, Vol. 56, pp. 239–246.
 10. E.F. Bratuta and S.F. Kravtsov, 1986, "The Effect of Subcooling of Dispersed Liquid on Critical Heat Flux with Cooling of a Plane Surface," *Thermal Engineering*, Vol. 33, pp. 674–676.